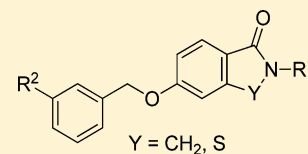


Orally Active Metabotropic Glutamate Subtype 2 Receptor Positive Allosteric Modulators: Structure–Activity Relationships and Assessment in a Rat Model of Nicotine Dependence

Shyama Sidique,^{†,‡,§} Raveendra-Panickar Dhanya,^{†,‡,§} Douglas J. Sheffler,^{||,#} Hilary Highfield Nickols,^{⊥,#} Li Yang,^{‡,§} Russell Dahl,^{‡,§} Arianna Mangravita-Novo,[§] Layton H. Smith,[§] Manoranjan S. D'Souza,[□] Svetlana Semenova,[□] P. Jeffrey Conn,^{||,#} Athina Markou,[□] and Nicholas D. P. Cosford^{*,‡,§}

[‡]Apoptosis and Cell Death Research Program and [§]Conrad Prebys Center for Chemical Genomics, Sanford-Burnham Medical Research Institute, 10901 N. Torrey Pines Road, La Jolla, California 92037, United States, Departments of ^{||}Pharmacology, [⊥]Pathology, Microbiology and Immunology, and [#]Vanderbilt Center for Neuroscience Drug Discovery, Vanderbilt University Medical Center, Nashville, Tennessee 37232, United States, and [□]Department of Psychiatry, School of Medicine, University of California San Diego, La Jolla, California 92093, United States

ABSTRACT: Compounds that modulate metabotropic glutamate subtype 2 (mGlu₂) receptors have the potential to treat several disorders of the central nervous system (CNS) including drug dependence. Herein we describe the synthesis and structure–activity relationship (SAR) studies around a series of mGlu₂ receptor positive allosteric modulators (PAMs). The effects of N-substitution (R¹) and substitutions on the aryl ring (R²) were identified as key areas for SAR exploration (Figure 3). Investigation of the effects of varying substituents in both the isoindolinone (2) and benzisothiazolone (3) series led to compounds with improved in vitro potency and/or efficacy. In addition, several analogues exhibited promising pharmacokinetic (PK) properties. Furthermore, compound 2 was shown to dose-dependently decrease nicotine self-administration in rats following oral administration. Our data, showing for the first time efficacy of an mGlu₂ receptor PAM in this in vivo model, suggest potential utility for the treatment of nicotine dependence in humans.



■ INTRODUCTION

Tobacco smoking causes significant preventable morbidity and mortality throughout the world.^{1,2} Unfortunately, smoking cessation medications currently approved by the Food and Drug Administration (FDA) are not effective in the majority of tobacco smokers who attempt to quit.³ Thus, there is a need to develop medications with novel mechanisms of action for smoking cessation. Nicotine is one of the major psychoactive components of tobacco that is considered to contribute to the initiation and maintenance of the tobacco smoking habit.⁴ Thus, a compound that attenuates the reinforcing effects of nicotine may be effective as a smoking cessation medication.

The excitatory neurotransmitter glutamate plays a critical role in mediating the reinforcing effects of nicotine.^{5–8} Nicotine increases glutamatergic neurotransmission by activating excitatory nicotinic acetylcholine (nACh) receptors located on presynaptic glutamatergic terminals. Therefore, a drug which indirectly blocks the effects of nicotine by antagonizing nicotine-induced increases in glutamate release may be as effective as a more direct acting agent such as bupropion. Glutamatergic neurotransmission is negatively regulated by Group II metabotropic glutamate (mGlu) receptors consisting of the mGlu₂ and mGlu₃ receptor subtypes.^{9,10} The mGlu₂ and mGlu₃ receptors perform a modulatory role during synaptic transmission by coupling to G_{i/o} proteins that negatively regulate the activity of adenylyl cyclase.¹¹ There is ample evidence demonstrating that repeated exposure to cocaine or nicotine alters mGlu₂ receptor function.^{12–14} Conversely, we have reported previously that the reinforcing effects

of nicotine were attenuated by LY379268, a competitive agonist that binds to both the mGlu₂ and mGlu₃ receptor subtypes.¹⁴ In the same study, however, LY379268 also attenuated responding to a natural reward, food, indicating a lack of selectivity of the effects of this compound for nicotine-maintained behaviors. One possible reason for this lack of selectivity may relate to the site of action of LY379268, specifically the orthosteric (glutamate) binding site of mGlu_{2/3} receptors. Compounds acting at the orthosteric site, such as LY379268, lack selectivity for mGlu₂ vs mGlu₃ receptors, presumably due to the high degree of sequence homology at the glutamate binding site.¹⁵ Alternatively, mGlu₂ receptor selectivity may be achieved by targeting less conserved allosteric sites on the receptor. Thus, a mGlu₂ receptor-selective positive allosteric modulator (PAM), such as the prototypical compound 3'-((2-cyclopentyl-6,7-dimethyl-1-oxo-2,3-dihydro-1H-inden-5-yloxy)methyl)biphenyl-4-carboxylic acid (BINA, 1), can noncompetitively potentiate the function of glutamate at mGlu₂ receptors.¹⁶

Several pharmaceutical companies have investigated mGlu₂ receptor PAMs for the potential treatment of schizophrenia or anxiety (comprehensively reviewed in ref 16). For example, scientists at Lilly,¹⁷ Merck,¹⁸ Pfizer,¹⁹ and Janssen^{20,21} have recently disclosed their work on the discovery and optimization of mGlu₂ receptor PAMs (Figure 1). We have reported our initial studies on the design, synthesis, and preliminary structure–activity

Received: April 14, 2012

Published: September 25, 2012

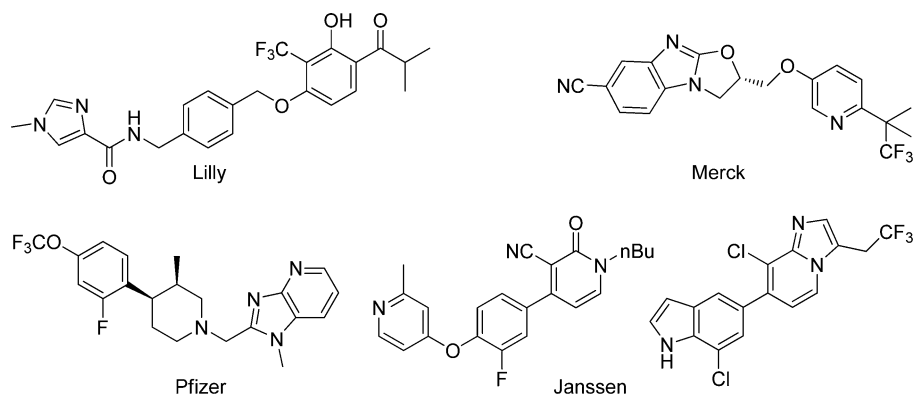


Figure 1. Structures of recently reported mGlu₂ receptor PAMs.

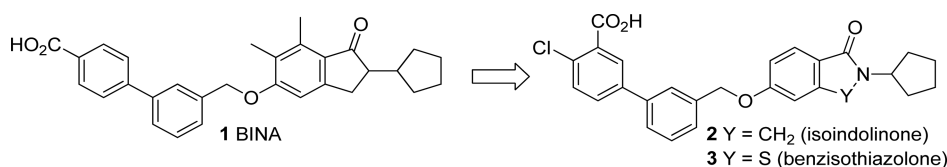


Figure 2. Structures of our mGlu₂ receptor PAMs.

relationships (SAR) around a series of mGlu₂ receptor PAMs that are systemically active following oral dosing in rats.²² Our studies were prompted by the fact that while compound **1** is selective and brain penetrant following ip dosing, it lacks potency for mGlu₂ receptors both in vitro and in vivo and has suboptimal pharmacokinetic (PK) properties. In the previous disclosure we described various modifications of the indanone ring of **1** including the incorporation of heteroatoms and expansion of the fused five-membered ring to a fused six-membered ring. In addition, it was found that the methyl substituents at positions 6 and 7 of the indanone moiety in compound **1** were not necessary for activity in the new series. Furthermore, compounds in the isoindolinone (**2**) and benzothiazolone (**3**) series (Figure 2) provided analogues with improved properties compared with BINA, including excellent brain levels after oral dosing in rats. In the present study, we investigated the effects on potency, efficacy, and druglike properties of different N-substituents (R¹) in the benzothiazolone series, and the effects of modifying the aryl substituents (R²) in the isoindolinone series (Figure 3).

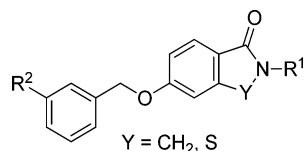


Figure 3. Areas of SAR investigation in the present study.

Our previous studies demonstrated that compounds **1**²³ and **3**²² (Figure 2), unlike mGlu_{2/3} receptor orthosteric agonists, decreased cocaine self-administration in rats at doses that did not affect responding for food.^{22,23} Herein, we report further investigations into the SAR around this series of compounds and the identification of additional potent mGlu₂ receptor PAMs with druglike properties. Importantly, in the present study we report for the first time the effects of an mGlu₂ receptor PAM in rats self-administering nicotine.

Chemistry. The synthesis of benzothiazolone analogues **3a-f** is illustrated in Scheme 1. Methyl 4-methoxythiosalicylate

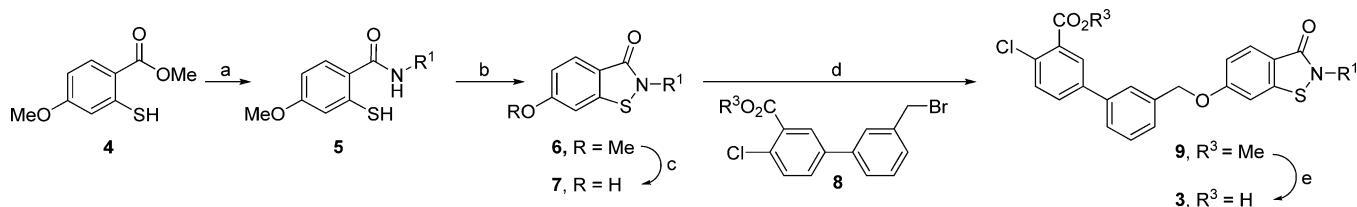
4 was converted to an amide derivative **5** by treatment with the corresponding amine in the presence of trimethylaluminum. Cyclization to access the benzothiazol-3-one derivative **6** was accomplished by a PIFA-mediated in situ formation of an N-acylnitrenium ion and its intramolecular trapping by the thiol moiety. Demethylation of **6** was achieved with BBr₃ in hot benzene to afford intermediate **7**. O-Alkylation of **7** with methyl 3'-(bromomethyl)-4-chlorobiphenyl-3-carboxylate (**8**) gave compound **9** which was saponified with lithium iodide to provide the target carboxylic acid derivatives **3a-f**.

To access analogues in which various aryl substituents (R², Figure 3) could be incorporated into the structure, we developed the synthetic route shown in Scheme 2. Thus, reaction of 3-(bromomethyl)phenylboronic acid (**12**) with either **10** or **11** provided the key intermediates **13** and **14**, respectively. Compounds **13** and **14** were then subjected to Suzuki cross-coupling conditions with substituted aryl halides to yield the corresponding isoindolinone derivatives **15a-k** and benzothiazolone analogue **16a**.

An alternative synthetic route was employed for the synthesis of benzothiazolone derivatives **16b** and **16c** which is shown in Scheme 3. Thus, benzothiazolone derivative **11** was reacted with 1-bromo-3-(bromomethyl)benzene (**17**) to provide the corresponding ether derivative **18**. Intermediate **18** was then subjected to Suzuki cross-coupling conditions with the appropriate arylboronic acid derivatives to provide the target compounds **16b** and **16c**.

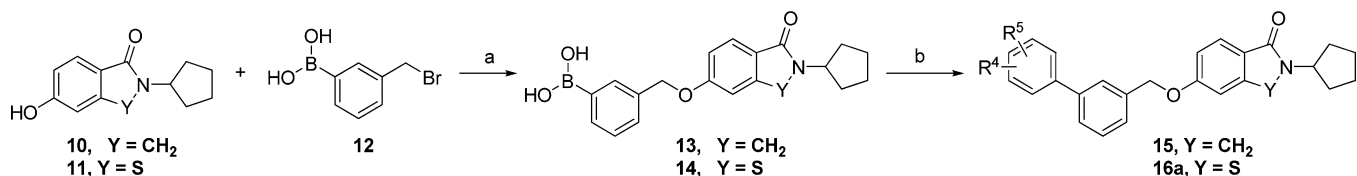
In the benzothiazolone series, compound **3** was converted to the dimethylamide derivative **19** as shown in Scheme 4. In addition, in the isoindolinone series the importance of the ether linker was investigated by preparing the analogue containing a triaryl moiety (**24**) (Scheme 5). The synthesis began with commercially available 4-bromo-2-methylbenzoic acid (**20**), which was esterified to provide **21**, brominated at the benzylic position to provide **22**, and converted to 5-bromo-2-cyclopentylisoindolin-1-one (**23**) using a previously described procedure.²⁴ Finally, two consecutive Suzuki couplings yielded 4-chloro-3'-(2-cyclopentyl-1-oxoisoindolin-5-yl)biphenyl-3-carboxylic acid **24**.

Scheme 1. Synthesis of 3-Chloro-3'-((2-cyclopentyl-3-oxo-2,3-dihydrobenzo[*d*]isothiazol-6-yloxy)methyl)biphenyl-4-carboxylic Acid Derivatives 3a–f^a



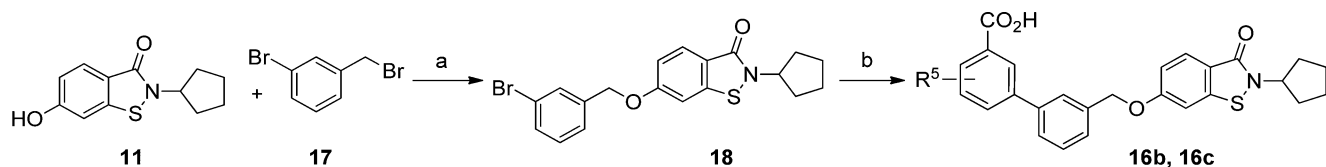
^aReagents and conditions: (a) AlMe₃, R¹NH₂, CH₂Cl₂, 0 °C to 60 °C, 12 h; (b) PIFA, TFA, 0 °C, CH₂Cl₂, 1 h; (c) (i) BBr₃, C₆H₆, 80 °C, 1 h; (ii) H₂O, 100 °C, 1 h; (d) ArCH₂Br, K₂CO₃, MeCN, 80 °C, 12 h; (e) LiI, pyridine, 110 °C, 12 h.

Scheme 2. General Synthetic Scheme for the Synthesis of Isoindolinones 15a–k and Benzoisothiazolone Analogue 16a^a



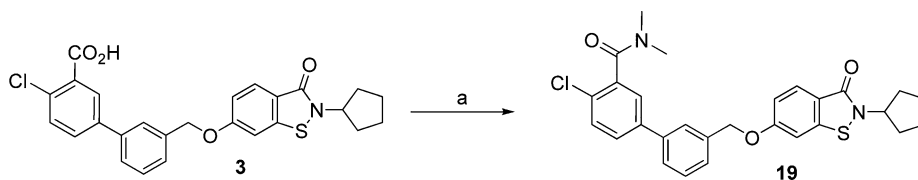
^aReagents and conditions: (a) K₂CO₃, acetone, reflux; (b) when Y = CH₂; RX, PdCl₂(PPh₃)₂, K₂CO₃, toluene/MeOH, 80 °C or when Y = S; RX, Pd(PPh₃)₄, DME, 80 °C, 12 h.

Scheme 3. Synthesis of Benzoisothiazolone Derivatives 16b and 16c^a



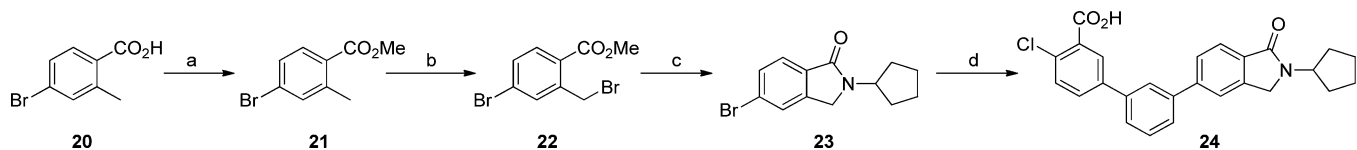
^aReagents and conditions: (a) K₂CO₃, CH₃CN, 80 °C, 1 h; (b) RB(OH)₂, Pd(PPh₃)₄, DME, 80 °C, 12 h.

Scheme 4. Synthesis of Amide Analogue 19^a



^aReagents and conditions: (a) HOBt, EDC-HCl, Me₂NH-HCl, Et₃N, DMF, rt, 3 h.

Scheme 5. Synthesis of Isoindolinone Analogue 24^a

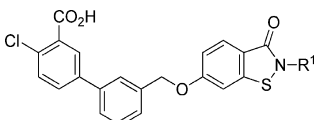


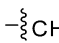
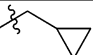
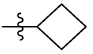
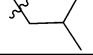
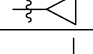
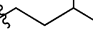
^aReagents and conditions: (a) MeOH, cat. H₂SO₄, reflux, 12 h; (b) NBS, cat. AIBN, CCl₄, 68 °C, 12 h; (c) C₅H₉NH₂, K₂CO₃, CH₃CN, reflux, 12 h; (d) (i) 3-bromophenylboronic acid, Pd(PPh₃)₄, 2 M Na₂CO₃, DME, reflux, 1 h; (ii) 5-borono-2-chlorobenzoic acid, Pd(PPh₃)₄, 2 M Na₂CO₃, DME, reflux, 2 h.

RESULTS AND DISCUSSION

The new analogues 3a–f, 15a–k, 16a–c, 19, and 24 were tested to determine *in vitro* activity, and the data are summarized in Tables 1 and 2. A thallium flux assay was performed in HEK-GIRK cells²⁵ expressing rat mGlu₂ receptors to determine potency and efficacy at the target receptors. The concentration–response relationship that potentiates the effect of an EC₂₀ concentration of glutamate was determined for each of

the mGlu₂ receptor PAMs, and the potency is expressed as an EC₅₀ value. Efficacy for the potentiation of an EC₂₀ concentration of glutamate is presented as a percentage of the maximal glutamate response. Also shown in Tables 1 and 2 are *in vitro* absorption, distribution, metabolism, and excretion (ADME) data for the analogues. We determined the stability of compounds *in vitro* in rat plasma and rat liver microsomes, in addition to membrane permeability using a parallel artificial membrane assay (PAMPA) to aid in predicting their *in vivo*

Table 1. In Vitro Data for Benzothiazolone mGlu₂ Receptor PAMs: Variation of R¹


Compound	R ¹	mGlu ₂ PAM EC ₅₀ (μM) ^a	% Glutamate Max ^a	Permeability (log P _c) ^b	Plasma stability ^{c,d}	Microsomal stability ^{c,d}
1 (BINA)		0.38 ± 0.13	83.2 ± 10.0	-6.2	66	20
2		0.05 ± 0.02	81.4 ± 11.7	-5.5	100	42
3		0.17 ± 0.03	63.0 ± 3.3	-5.4	86	45
3a		0.64 ± 0.06	74.7 ± 1.7	-5.3	100	84
3b		2.48 ± 0.77	38.4 ± 1.0	-7.1	100	75
3c		0.58 ± 0.08	83.0 ± 1.5	-5.4	91	67
3d		0.47 ± 0.04	76.2 ± 2.0	-5.0	95	86
3e		0.13 ± 0.01	70.6 ± 1.7	-5.5	100	86
3f		0.65 ± 0.03	67.3 ± 0.6	-7.5	91	92

^amGlu₂ receptor PAM EC₅₀ (μM) data and % glutamate max data represent the mean ± SEM for at least three independent experiments performed in triplicate. ^bPermeability is monitored by measuring the amount of compound that can diffuse through a polar brain lipid membrane to predict BBB permeability.²⁶ ^cPercent remaining after incubation for 60 min at 37 °C. NT = not tested. ^dSpecies = rat.

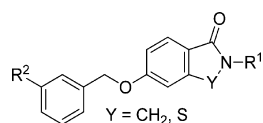
pharmacological profiles. Compounds with a permeability value (log P_c) of around -5.5 in the CNS PAMPA assay are likely to be brain penetrant.

Analysis of the data in Tables 1 and 2 showed that in the benzisothiazolone series, variation of R¹ did not significantly improve potency compared with 3 (compounds 3a–f, Table 1); however, 3e was slightly more potent and efficacious than 3 and had improved rat plasma and rat microsomal stability. In the isoindolinone series (compounds 15a–f, Table 2), introduction of methoxy or hydroxyl substituents into the R² benzoic acid moiety led to compounds with excellent potency and efficacy (15a–c). For example, replacement of the chloro substituent in compound 2 with a hydroxyl group, as in 15b, resulted in improved mGlu₂ potency but with loss of microsomal stability (Table 2). Introduction of halide or methyl substituents into the R² benzoic acid moiety (as in 15d–g) provided analogues with good potency (100 nM range for EC₅₀) and efficacy. In the benzothiazolone series, introduction of substituents into the R² benzoic acid moiety (as in 16a–c) did not lead to a significant potency enhancement. Furthermore, conversion of the carboxylic acid moiety in 3 to the dimethylamide derivative (19) led to a 6-fold potency reduction. Isoindolinone analogues lacking the carboxylic acid moiety in R² (15i–k) were essentially inactive in vitro, demonstrating the importance of the carboxylic acid moiety in R² in this series. Finally, replacement of the oxymethylene bridge between the oxoisindoline and biphenyl moieties of compound 2 with a single bond provided compound 24 with a 3-fold improvement in mGlu₂ potency and excellent plasma and microsomal stability in vitro.

As shown in Tables 1 and 2, several of the new analogues displayed superior druglike properties compared with 1, suggesting that these improvements may translate to in vivo efficacy. Compounds 3e, 15a, and 24 were selected for profiling against other mGlu receptor subtypes to determine the relative selectivity for

mGlu₂ receptors (Table 3). Overall the compounds were found to be highly selective for mGlu₂ receptors vs other subtypes. Thus, in general compounds 3e, 15a and 24 were >200-, >300-, and >1000-fold selective respectively for mGlu₂ compared with other mGlu receptor subtypes. The exceptions were compound 15a, which exhibited weak PAM activity against mGlu₃, and compound 24, which exhibited weak PAM activity against mGlu₇. As representatives of the respective series, compounds 2 and 3 were also profiled in binding assays against a comprehensive panel of CNS receptors through the NIMH Psychoactive Drug Screening Program (PDSP; see <http://pdsp.med.unc.edu/indexR.html> for details) and additional targets at Ricerca Biosciences. As shown in Table 4, at a concentration of 10 μM, overall neither 2 nor 3 exhibited significant activity against the majority of the targets. Compound 2 exhibited >50% activity at α_{1A}, α_{1D}, and H₁ receptors and the cytochrome P450 isozyme (CYP) 2C9. Testing in dose–response mode provided the following IC₅₀ values for compound 2: α_{1A} = 8.15 μM; α_{1D} > 10 μM; H₁ = 8.15 μM; CYP 2C9 = 8.2 μM. On the other hand, compound 3 had a single significant interaction at rat brain benzodiazepine receptors (IC₅₀ = 2.35 μM) but at 10 μM inhibited all the CYPs tested except for CYP 2D6. Dose–response testing yielded the following IC₅₀ values for compound 3 in the CYP panel: 1A2 = 6.2 μM; 2C9 = 4.0 μM; 3A4 > 25 μM.

In Vivo Pharmacokinetics. On the basis of the overall in vitro profile of the compounds in Tables 1–4, isoindolinone derivatives (2, 15a, 15b, 24) and a benzothiazolone derivative (3e) were selected for an in vivo assessment of their PK properties in rats. To optimize their solubility and improve gastrointestinal absorption, the compounds were converted to the corresponding sodium salts for the PK studies. The rat PK data for compounds 2, 3e, 15a, 15b, and 24 are shown in Table 5 (oral dosing) and Table 6 (intravenous or intraperitoneal dosing).

Table 2. In Vitro Data for mGlu₂ Receptor PAMs

Compound	Y	R ²	mGlu ₂ PAM EC ₅₀ (μM) ^a	% Glutamate Max ^a	Permeability (log P _o) ^b	Plasma stability ^{c,d}	Microsomal stability ^{c,d}
15a	CH ₂		0.08 ± 0.02	79.2 ± 1.6	-5.6	100	30
15b	CH ₂		0.02 ± 0.01	90.1 ± 1.5	-6.5	98	9
15c	CH ₂		0.08 ± 0.01	95.3 ± 2.6	-5.5	96	29
15d	CH ₂		0.09 ± 0.02	93.9 ± 2.0	-5.9	100	15
15e	CH ₂		0.11 ± 0.02	89.4 ± 0.8	-6.5	100	3
15f	CH ₂		0.11 ± 0.02	80.8 ± 0.6	-5.8	100	2
15g	CH ₂		0.13 ± 0.03	80.8 ± 1.9	-6.0	95	55
15h	CH ₂		0.17 ± 0.02	78.0 ± 2.7	-5.6	100	84
15i	CH ₂		> 5	ND	-6.9	95	38
15j	CH ₂		> 5	ND	NT	NT	NT
15k	CH ₂		> 5	ND	NT	NT	NT
16a	S		0.74 ± 0.08	82.9 ± 1.9	-5.4	100	92
16b	S		0.20 ± 0.02	86.1 ± 4.5	-7.7	100	84
16c	S		0.24 ± 0.02	83.4 ± 3.2	-5.4	100	71
19	S		0.98 ± 0.02	54.8 ± 4.0	-5.7	100	92
24	CH ₂		0.02 ± 0.01	85.8 ± 1.5	-5.7	81	70

^amGlu₂ receptor PAM EC₅₀ μM data and % glutamate max data represent the mean ± SEM for at least three independent experiments performed in triplicate. ^bPermeability is monitored by measuring the amount of compound that can diffuse through a polar brain lipid membrane to predict BBB permeability.²⁶ ^cPercent remaining after incubation for 60 min at 37 °C. NT = not tested. ND = not determined. ^dSpecies = rat.

All compounds were found to be systemically bioavailable with a long half-life (*t*_{1/2}) when dosed orally (Table 5). For example, compounds 2, 3e, 15a, and 15b exhibited micromolar plasma

levels when dosed orally. Overall the PK data for compound 24 were inferior, with low C_{max} and AUC values, suggesting that this compound would be a poor choice for further studies. In

Table 3. mGlu Receptor Subtype Selectivity^a

mGlu receptor subtype	compd 3e (EC ₅₀ μM)	compd 15a (EC ₅₀ μM)	compd 24 (EC ₅₀ μM)
mGlu ₁	>30	>30	>30
mGlu ₃	>30	PAM	>30
mGlu ₄	>30	>30	>30
mGlu ₅	>30	>30	>30
mGlu ₆	>30	>30	>30
mGlu ₇	>30	>30	PAM
mGlu ₈	>30	>30	>30

^aIn these selectivity experiments, for all receptors a full concentration-response of agonist was performed once in triplicate in the presence and absence of a 10 μM final concentration of each compound. Where 10 μM compound caused more than a 2 fold shift of the glutamate concentration–response curve, full concentration–response curves were performed in triplicate on three different days to assess potency of compounds. Compound 15a showed weak potentiator activity at mGlu₃, and compound 24 showed weak potentiator activity at mGlu₇.

addition, compound 15a had high clearance (C_L) and volume of distribution (V_d) values, indicating rapid metabolism coupled with sequestration into other compartments (e.g., fatty tissue). On the other hand, compounds 2, 3e, and 15b had low V_d and

C_L (2 and 15b) values, suggesting that these compounds might be promising candidates for in vivo studies. Furthermore, compounds 2, 15a, and 15b possessed excellent oral bioavailability (%F). Consequently, brain levels were determined for compounds 2, 3e, 15a, and 15b following a 10 mg/kg oral dose and the brain concentrations were compared to the in vitro mGlu₂ PAM EC₉₀ values for each compound (Table 5). These data revealed that only compound 2 achieved brain levels (236 nM at 10 mg/kg po) consistent with its mGlu₂ PAM EC₉₀ value (237 nM), suggesting that at this oral dose or above, the majority of the target receptors would be activated in the brain. Taking all the relevant data into account, compound 2 was therefore selected for behavioral studies in rats.

Behavioral Studies. The in vivo model was designed to assess the effects of acute systemic (oral) administration of compound 2 as its sodium salt on the reinforcing effects of nicotine using the intravenous nicotine self-administration procedure in rats. This in vivo test is considered one of the most direct and reliable measures of the reinforcing properties of nicotine in an animal model.⁶ Nicotine self-administration sessions were 1 h long (see Experimental Section for details). The results of the in vivo behavioral studies are shown in Figure 4. Oral administration of compound 2 significantly decreased nicotine self-administration in rats compared to vehicle treatment at doses of

Table 4. Off-Target Profiling Data for Compounds 2 and 3^a

receptor/target	species	compd 2, % inhibition ^b	compd 3, % inhibition ^b	receptor/target	species	compd 2, % inhibition ^b	compd 3, % inhibition ^b
adrenergic α _{1A}	human	65 (8.15 μM)	2	muscarinic M ₅	human	20	27
adrenergic α _{1B}	human	44	8	opiate δ (OP1, DOP)	human	37	23
adrenergic α _{1D}	human	52 (>10 μM)	3	opiate κ (OP2, KOP)	human	–23	–12
adrenergic α _{2A}	human	–1	31	opiate μ (OP3, MOP)	human	41	38
adrenergic α _{2B}	human	22	18	serotonin (5-hydroxytryptamine) 5-HT _{1A}	human	0.1	6
adrenergic α _{2C}	human	24	30	serotonin (5-hydroxytryptamine) 5-HT _{1B}	human	–7	–3
adrenergic β ₁	human	–2	–1	serotonin (5-hydroxytryptamine) 5-HT _{1D}	human	–9	–14
adrenergic β ₂	human	8	4	serotonin (5-hydroxytryptamine) 5-HT _{1E}	human	6	–14
adrenergic β ₃	human	21	13	serotonin (5-hydroxytryptamine) 5-HT _{2A}	human	20	46
benzodiazepine (brain, [³ H]flunitrazepam)	rat	34	51 (2.35 μM)	serotonin (5-hydroxytryptamine) 5-HT _{2B}	human	9	0
calcium channel L-type, dihydropyridine ^c	rat	–2	22	serotonin (5-hydroxytryptamine) 5-HT _{2C}	human	18	–12
cytochrome P450, 1A2 ^c	human	14	100 (6.2 μM)	serotonin (5-hydroxytryptamine) 5-HT ₃	human	10	–13
cytochrome P450, 2C9 ^c	human	92 (8.2 μM)	93 (4.0 μM)	serotonin (5-hydroxytryptamine) 5-HT _{5A}	human	19	7
cytochrome P450, 2D6 ^c	human	10	42	serotonin (5-hydroxytryptamine) 5-HT ₆	human	14	16
cytochrome P450, 3A4 ^c	human	40	94 (>25 μM)	serotonin (5-hydroxytryptamine) 5-HT ₇	human	11	10
dopamine D ₁	human	32	50 (>10 μM)	sigma σ ₁	rat	25	33
dopamine D ₂	human	10	2	sigma σ ₂	rat	42	–2
dopamine D ₃	human	–9	6	transporter, dopamine (DAT)	human	40	12
dopamine D ₄	human	10	3	transporter, norepinephrine (NET)	human	4	–17
dopamine D ₅	human	15	28	transporter, serotonin (5-hydroxytryptamine) (SERT)	human	6	8
GABA _A (brain, [³ H]muscimol)	rat	–14	–10				
histamine H ₁	human	59 (8.15 μM)	56 (>10 μM)				
histamine H ₂	human	27	29				
histamine H ₃	guinea pig	14	–9				
histamine H ₄	human	4	1				
muscarinic M ₁	human	2	3				
muscarinic M ₂	human	–10	20				
muscarinic M ₃	human	–2	7				
muscarinic M ₄	human	–7	8				

^aCompounds were tested for displacement of radioligand binding activity at 10 μM. Assays were performed by the NIMH Psychoactive Drug Screening Program (UNC Chapel Hill) unless otherwise noted. ^bInhibition at 10 μM as a percentage of displacement of the respective radioligand at each target. IC₅₀ values where applicable are shown in parentheses. ^cAssay screen at 10 μM performed by Ricerca Biosciences. Assays to determine IC₅₀ values were performed by the Sanford-Burnham Exploratory Pharmacology Core.

Table 5. In Vivo PK Data for mGlu₂ Receptor PAMs (as sodium salts) after Oral Administration in Rats^a

compd	C _{max} (μM)	T _{max} (min)	V _d (mL)	AUC (0–t) (μmol·min/mL)	t _{1/2} (h)	F (%)	mGlu ₂ PAM EC ₉₀ (μM)	brain ^b (μM)	plasma ^b (μM)	brain:plasma ratio
2 ^c	3 ± 0.1	120	3.0	2552	7	71.4 ± 2.3	0.237	0.236 ± 0.022	6.18 ± 0.869	0.039 ± 0.002
3e ^c	8.5 ± 3.04	60	4.1	3690	8.6	ND	0.664	0.03 ± 0.01	0.8 ± 0.2	0.04 ± 0.01
15a ^c	4 ± 2.9	30	10875.2	0.72	16.25	84.8 ± 8.9	0.248	0.18 ± 0.01	1.46 ± 0.29	0.13 ± 0.03
15b ^c	1.6 ± 0.4	30	28.0	426.0	10.6	109.2 ± 9.1	0.102	0.0071 ± 0.0004	0.21 ± 0.046	0.0335 ± 0.015
24 ^c	0.4 ± 0.2	30	96.2	0.16	3.06	ND	ND	ND	ND	ND

^aOral dose: 10 mg/kg; vehicle: sterile water. ^bBrains and plasma were harvested at or near the T_{max}. ^cNumber of animals used for 2, 3e, 15a, and 24, n = 3, for 15b, n = 5. C_{max}: maximum concentration of the compound detected in plasma. T_{max}: time at C_{max}. V_d: volume of distribution. AUC: area under the curve. t_{1/2}: terminal half-life. F: oral bioavailability. ND: not determined.

Table 6. In Vivo PK Data for mGlu₂ PAMs (as sodium salts) in Rats after Intravenous or Intraperitoneal Administration

compd	C _{max} (μM)	C _L (mL/min)	V _d (mL)	AUC (0–t) (μmol·min/mL)	t _{1/2} (h)
2 ^a	28.2 ± 1.1	0.006	0.6	710.2	1.5
3e ^b	9.6 ± 6.1	ND	2.4	1549.3	11.2
15a ^a	5.6 ± 1.8	9.7	4620.0	0.4	0.51
15b ^a	3.9 ± 0.6	0.028	4.3	154.4	1.8
24 ^b	2.0 ± 0.2	ND	21.2	193.6	2.01

^aIntravenous dose 2 mg/kg, vehicle used: sterile water. ^bIntraperitoneal dose 10 mg/kg, vehicle used: sterile water. C_{max}: maximum concentration of compound detected in plasma. C_L: clearance. V_d: volume of distribution. AUC: area under the curve. t_{1/2}: terminal half-life.

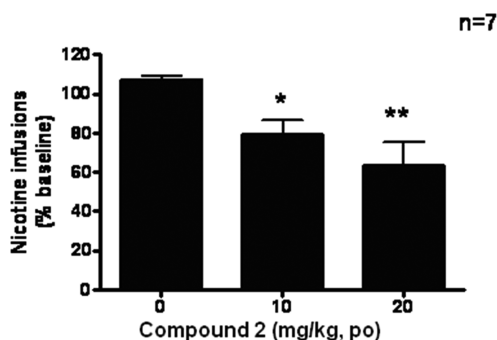


Figure 4. Effects of compound 2 on nicotine self-administration in rats. Data are expressed as percent of baseline number of infusions earned (mean ± SEM). The number of baseline nicotine infusions was 13.88 ± 1.62 (mean ± SEM). **p* < 0.05, ***p* < 0.01, significant differences from the corresponding vehicle condition (Newman–Keuls posthoc test after a significant main effect in the ANOVA).

10 and 20 mg/kg (Figure 4). These results demonstrate that mGlu₂ receptor PAMs may be useful therapeutically for the treatment of nicotine dependence.

In conclusion, expansion of the SAR around the prototypical mGlu₂ receptor PAM (1) led to additional potent and efficacious analogues. These compounds are highly selective for mGlu₂ vs other mGlu receptor subtypes and also vs other CNS receptors. Several analogues (2, 3e, 15a, and 15b) have promising in vitro ADME and in vivo PK properties, providing compounds with excellent oral bioavailability and adequate brain penetration. The potent mGlu₂ receptor PAM (2) was shown to reduce nicotine infusions by 40% at a dose of 20 mg/kg po in a rat model, providing proof-of-concept for the use of an orally active mGlu₂ receptor PAM for the treatment of nicotine addiction.

EXPERIMENTAL SECTION

General Chemistry. All reactions were performed in oven-dried glassware under an atmosphere of argon with magnetic stirring. All solvents and chemicals used were purchased from Sigma-Aldrich or Acros and were used as received without further purification. Purity and characterization of compounds were established by a combination of liquid chromatography–mass spectroscopy (LC-MS) and NMR analytical techniques and was >95% for all tested compounds. Silica gel column chromatography was carried out using prepacked silica cartridges from RediSep (ISCO Ltd.) and eluted using an Isco Companion system. ¹H and ¹³C NMR spectra were obtained on a Jeol 400 spectrometer at 400 and 100 MHz, respectively, unless otherwise mentioned. Chemical shifts are reported in δ (ppm) relative to residual solvent peaks or TMS as internal standards. Coupling constants are reported in hertz. High-resolution ESI-TOF mass spectra were acquired from the Mass Spectrometry Core at The Sanford-Burnham Medical Research Institute (Orlando, FL). HPLC-MS analyses were performed on a Shimadzu 2010EV LCMS using the following conditions: Kromasil C18 column (reverse phase, 4.6 mm × 50 mm); a linear gradient from 10% acetonitrile and 90% water to 95% acetonitrile and 5% water over 4.5 min; flow rate of 1 mL/min; UV photodiode array detection from 200 to 300 nm.

Compounds 3a–f were prepared in a similar manner to the procedure previously described for 4-chloro-3'-((2-cyclopentyl-3-oxo-2,3-dihydrobenzo[d]isothiazol-6-yloxy)methyl)biphenyl-3-carboxylic acid.²²

4-Chloro-3'-((2-methyl-3-oxo-2,3-dihydrobenzo[d]isothiazol-6-yloxy)methyl)biphenyl-3-carboxylic Acid (3a). Colorless solid (70 mg, 52%). ¹H NMR (400 MHz, DMSO-*d*₆): δ 8.01 (s, 1H), 7.84–7.79 (m, 3H), 7.72 (d, 1H, *J* = 8.5 Hz), 7.60 (s, 1H), 7.58 (d, 1H, *J* = 8.6 Hz), 7.49–7.47 (m, 2H), 7.05 (d, 1H, *J* = 8.5 Hz), 5.23 (s, 2H), 3.24 (s, 3H). ¹³C NMR (100 MHz, DMSO-*d*₆): δ 167.8, 164.8, 161.2, 144.1, 138.8, 138.3, 137.7, 132.1, 131.4, 130.9, 130.6, 129.5, 128.7, 127.6, 126.4, 126.2, 125.7, 115.5, 106.9, 70.8, 32.0. LC-MS (ESI) Calcd for C₂₂H₁₆ClNO₄S [M + H]⁺: 426.05. Found: 425.90. HRMS (ESI) calcd for C₂₂H₁₆ClNO₄S [M + H]⁺: 426.0561; found: 426.0553.

4-Chloro-3'-((2-cyclopropylmethyl)-3-oxo-2,3-dihydrobenzo[d]isothiazol-6-yloxy)methyl)biphenyl-3-carboxylic Acid (3b). Pale yellow solid (44 mg, 30%). ¹H NMR (400 MHz, DMSO-*d*₆): δ 8.11 (s, 1H), 7.98 (d, 1H, *J* = 8.5 Hz), 7.80 (d, 1H, *J* = 8.6 Hz), 7.71–7.76 (m, 4H), 7.49–7.47 (m, 2H), 7.07 (d, 1H, *J* = 8.5 Hz), 5.23 (s, 2H), 3.33 (d, 2H, *J* = 6.9 Hz), 1.06–0.98 (m, 1H), 0.53–0.51 (m, 2H), 0.35–0.32 (m, 2H). ¹³C NMR (100 MHz, DMSO-*d*₆): δ 167.4, 164.4, 162.2, 144.4, 139.8, 138.8, 131.6, 131.2, 130.7, 129.9, 128.3, 127.3, 126.9, 126.0, 124.7, 115.6, 106.6, 70.2, 48.0, 11.3.6, 4.3. LC-MS (ESI) Calcd for C₂₅H₂₀ClNO₄S [M + H]⁺: 466.08. Found: 465.95. HRMS (ESI) calcd for C₂₅H₂₀ClNO₄S [3M + H]⁺: 1398.2471; found: 1398.2853.

4-Chloro-3'-((2-cyclobutyl-3-oxo-2,3-dihydrobenzo[d]isothiazol-6-yloxy)methyl)biphenyl-3-carboxylic Acid (3c). Pale yellow solid (53 mg, 35%). ¹H NMR (400 MHz, CDCl₃): δ 8.01 (s, 1H), 7.82 (d, 1H, *J* = 8.5 Hz), 7.80 (d, 1H, *J* = 8.6 Hz), 7.71–7.76 (m, 4H), 7.49–7.47 (m, 2H), 7.05 (d, 1H, *J* = 8.5 Hz), 5.17 (s, 2H), 4.63–4.60 (m, 1H), 2.38–2.22 (m, 2H), 2.04–2.02 (m, 2H), 1.37–1.33 (m, 2H). ¹³C NMR (100 MHz, CDCl₃): δ 166.8, 165.2, 163.3, 147.0, 139.1, 138.8, 136.6, 132.2, 130.8, 129.0, 126.9, 126.5, 125.8, 119.8, 110.6, 70.3, 47.0, 29.7, 15.6. LC-MS (ESI) Calcd for C₂₅H₂₀ClNO₄S

[M + H]⁺: 466.08. Found: 465.90. HRMS (ESI) Calcd for C₂₅H₂₀ClNO₄S [2M + H]⁺: 931.1676. Found: 931.1629.

4-Chloro-3'-((2-isobutyl-3-oxo-2,3-dihydrobenzo[d]isothiazol-6-yloxy)methyl)biphenyl-3-carboxylic Acid (3d). Pale yellow solid (97 mg, 65%). ¹H NMR (400 MHz, CDCl₃): δ 8.05 (s, 1H), 7.84–7.80 (m, 1H), 7.56–7.38 (m, 6H), 7.21 (d, 1H, J = 8.4 Hz), 6.98 (d, 1H, J = 8.5 Hz), 5.17 (s, 2H), 3.58 (d, 2H, J = 7.3 Hz), 2.07–1.96 (m, 1H), 0.88 (d, J = 6.7 Hz, 6H). ¹³C NMR (100 MHz, CDCl₃): δ 167.5, 165.5, 163.5, 147.9, 143.2, 139.7, 138.9, 131.5, 130.7, 130.2, 129.4, 127.8, 127.0, 126.0, 115.1, 110.6, 70.8, 51.1, 22.9. LC-MS (ESI) Calcd for C₂₅H₂₂ClNO₄S [M + H]⁺: 468.09. Found: 467.90. HRMS (ESI) Calcd for C₂₅H₂₂ClNO₄S [M + H]⁺: 468.1031. Found: 468.1012.

4-Chloro-3'-((2-cyclopentyl-3-oxo-2,3-dihydrobenzo[d]isothiazol-6-yloxy)methyl)biphenyl-3-carboxylic Acid (3e). Pale yellow solid (43 mg, 30%). ¹H NMR (400 MHz, DMSO-*d*₆): δ 8.01 (s, 1H), 7.82–7.80 (m, 3H), 7.69 (d, 1H, J = 8.6 Hz), 7.60 (d, 1H, J = 8.5 Hz), 7.53–7.40 (m, 3H), 7.06 (d, 1H, J = 8.6 Hz), 5.23 (s, 2H), 3.00–2.98 (m, 1H), 0.96–0.92 (m, 2H), 0.87–0.83 (m, 2H). ¹³C NMR (100 MHz, DMSO-*d*₆): δ 167.7, 164.8, 161.2, 144.1, 138.8, 138.3, 137.7, 132.1, 131.4, 130.9, 130.6, 129.5, 128.7, 127.6, 126.4, 126.2, 125.7, 124.0, 115.5, 106.9, 70.2, 5.2. LC-MS (ESI) Calcd for C₂₄H₁₈ClNO₄S [M + H]⁺: 452.06. Found: 451.85. HRMS (ESI) Calcd for C₂₄H₁₈ClNO₄S [M + H]⁺: 452.0718. Found: 452.0716.

4-Chloro-3'-((2-isopentyl-3-oxo-2,3-dihydrobenzo[d]isothiazol-6-yloxy)methyl)biphenyl-3-carboxylic Acid (3f). Pale yellow solid (83 mg, 55%). ¹H NMR (400 MHz, DMSO-*d*₆): δ 8.02 (s, 1H), 7.84–7.82 (m, 4H), 7.79 (d, 1H, J = 8.5 Hz), 7.58 (d, 1H, J = 8.6 Hz), 7.49–7.47 (m, 2H), 7.05 (d, 1H, J = 8.5 Hz), 5.32 (s, 2H), 3.76–3.72 (m, 2H), 1.51–1.48 (m, 3H), 0.86 (d, J = 6.1 Hz, 6H). ¹³C NMR (100 MHz, DMSO-*d*₆): δ 167.8, 165.3, 149.7, 139.1, 137.8, 131.7, 131.0, 130.9, 129.9, 129.2, 127.5, 127.1, 126.9, 120.7, 112.0, 71.0, 54.8, 38.3, 25.7, 22.7. LC-MS (ESI) Calcd for C₂₆H₂₄ClNO₄S [M + H]⁺: 482.11. Found: 482.00. HRMS (ESI) Calcd for C₂₆H₂₄ClNO₄S [M + H]⁺: 482.1187. Found: 482.1173.

3'-((2-Cyclopentyl-1-oxoisindolin-5-yloxy)methyl)phenylboronic Acid (13). To a solution of 2-cyclopentyl-5-hydroxyisindolin-1-one (500 mg, 2.3 mmol) in acetone (20 mL) were added K₂CO₃ (1.2 g, 8.7 mmol) and 3-(bromomethyl)phenylboronic acid (650 mg, 3.0 mmol), and the mixture was heated with stirring at reflux for 3 h. The reaction mixture was filtered, and the solvent was evaporated in vacuo to obtain 3'-((2-cyclopentyl-1-oxoisindolin-5-yloxy)methyl)phenylboronic acid as a white solid (583 mg, 72%). The crude product was used for the next step without further purification. ¹H NMR (400 MHz, DMSO-*d*₆): δ 7.86 (s, 1H), 7.75–7.69 (m, 2H), 7.55–7.32 (m, 4H), 7.19 (s, 1H), 7.09–7.07 (m, 1H), 5.15 (s, 2H), 4.55–4.49 (m, 1H), 4.37 (s, 2H), 1.84–1.56 (m, 8H). LRMS calcd for C₂₀H₂₂BNO₄ [M + H]⁺ 352 found: 352.

3'-((2-Cyclopentyl-3-oxo-2,3-dihydrobenzo[d]isothiazol-6-yloxy)methyl)phenylboronic Acid (14). Potassium carbonate (166 mg, 1.2 mmol) was added to a solution of 2-cyclopentyl-7-hydroxy-3,4-dihydroisquinolin-1(2H)-one (235 mg, 1 mmol) and 3-(bromomethyl)phenylboronic acid (257 mg, 1.2 mmol) in acetone (10 mL). After being stirred for 1 h at 60 °C, the reaction mixture was cooled to room temperature and filtered. The filtrate was evaporated under reduced pressure to give crude 3'-((2-cyclopentyl-3-oxo-2,3-dihydrobenzo[d]isothiazol-6-yloxy)methyl)phenylboronic acid as a colorless solid (315 mg, 85%). The crude product was used for the next step without further purification. ¹H NMR (400 MHz, DMSO-*d*₆): δ 8.12 (s, 2H), 7.83 (s, 1H), 7.73–7.68 (m, 2H), 7.56 (s, 1H), 7.47 (d, 1H, J = 7.8 Hz), 7.32 (t, 1H, J = 7.8 Hz), 7.04 (d, 1H, J = 8.7 Hz), 5.25 (s, 2H), 4.85–4.81 (m, 1H), 2.01–1.98 (m, 2H), 1.75–1.59 (m, 6H). ¹³C NMR (100 MHz, DMSO-*d*₆): δ 164.4, 162.2, 143.3, 136.6, 134.4, 130.0, 128.8, 127.7, 115.6, 108.8, 70.8, 54.8, 32.2, 24.4. LC-MS (ESI) Calcd for C₁₉H₂₀BNO₄S [M + H]⁺: 370.12. Found: 369.90.

3'-((2-Cyclopentyl-1-oxoisindolin-5-yloxy)methyl)-6-methoxybiphenyl-3-carboxylic Acid (15a). 3'-((2-Cyclopentyl-1-oxoisindolin-5-yloxy)methyl)phenylboronic acid (100 mg, 0.28 mmol), 3-iodo-4-methoxybenzoic acid (67 mg, 0.24 mmol), K₂CO₃ (83 mg, 0.6 mmol), and PdCl₂(PPh₃)₂ (22 mg, 0.03 mmol) were dissolved in a mixture of toluene and MeOH (3.7:0.37 mL) and heated at 80 °C

for 1.5 h. The mixture was filtered through Celite and washed with water, and the solvents were removed in vacuo. The resulting crude material was acidified with 2 M HCl, extracted into EtOAc, and dried over anhydrous Na₂SO₄. The solvent was evaporated in vacuo to obtain the crude acid which was purified using automated preparative HPLC to yield the desired compound (33 mg, 30%) as a white solid. ¹H NMR (400 MHz, DMSO-*d*₆): δ 7.93 (d, J = 8.2 Hz, 1H), 7.82 (s, 1H), 7.55–7.42 (m, 5H), 7.21–7.18 (m, 2H), 7.10 (dd, J = 8.7 Hz, J = 2.3 Hz, 1H), 5.23 (s, 2H), 4.54–4.46 (m, 1H), 4.37 (s, 2H), 3.84 (s, 3H), 1.85–1.80 (m, 2H), 1.71–1.56 (m, 6H). ¹³C NMR (100 MHz, DMSO-*d*₆): δ 167.1, 166.8, 161.0, 159.5, 143.9, 137.5, 136.6, 131.5, 130.8, 129.2, 128.8, 128.4, 128.3, 126.6, 125.5, 123.9, 115.3, 111.5, 109.1, 69.5, 55.9, 51.9, 45.6, 29.6, 23.8. HRMS: calcd for C₂₈H₂₇NO₅ [M + H]⁺ 458.1962; found 458.1947.

3'-((2-Cyclopentyl-1-oxoisindolin-5-yloxy)methyl)-4-hydroxybiphenyl-3-carboxylic Acid (15b). White solid (18 mg, 20%). ¹H NMR (400 MHz, DMSO-*d*₆): δ 8.03 (dd, J = 7.3 Hz, J = 2.3 Hz, 1H), 7.85–7.39 (m, 6H), 7.24–6.94 (m, 3H), 5.24 (s, 2H), 4.55–4.47 (m, 1H), 4.37 (s, 2H), 1.86–1.56 (m, 8H). ¹³C NMR (100 MHz, DMSO-*d*₆): δ 171.7, 166.8, 161.0, 160.6, 143.9, 139.2, 137.4, 133.9, 130.9, 129.2, 127.9, 126.4, 125.8, 125.5, 123.8, 117.9, 115.3, 109.1, 69.5, 51.9, 45.6, 29.6, 23.8. HRMS calcd for C₂₇H₂₅NO₅ [M + H]⁺ 444.1805; found: 444.1800.

3'-((2-Cyclopentyl-1-oxoisindolin-5-yloxy)methyl)-2,6-dimethoxybiphenyl-4-carboxylic Acid (15c). White solid (8 mg, 16%). ¹H NMR (400 MHz, DMSO-*d*₆): δ 7.55 (d, J = 8.2 Hz, 1H), 7.40–7.09 (m, 8H), 5.19 (s, 2H), 4.56–4.48 (m, 1H), 4.39 (s, 2H), 3.69 (s, 6H), 2.02–1.54 (m, 8H). ¹³C NMR (100 MHz, DMSO-*d*₆): δ 167.1, 166.9, 161.1, 156.9, 143.9, 135.9, 133.5, 129.7, 127.8, 125.4, 123.8, 122.5, 115.6, 115.3, 109.1, 105.1, 69.6, 55.8, 51.9, 45.6, 29.6, 23.8. HRMS calcd for C₂₉H₂₉NO₆ [M + H]⁺ 488.2068; found: 488.2061.

6-Chloro-3'-((2-cyclopentyl-1-oxoisindolin-5-yloxy)methyl)biphenyl-3-carboxylic Acid (15d). White solid (8.2 mg, 14%). ¹H NMR (400 MHz, CDCl₃): δ 8.05 (s, 1H), 7.99–7.97 (m, 1H), 7.75 (d, J = 8.2 Hz, 1H), 7.55–7.41 (m, 5H), 7.06–7.04 (m, 1H), 6.99 (s, 1H), 5.17 (s, 2H), 4.77–4.69 (m, 1H), 4.28 (s, 2H), 1.99–1.55 (m, 8H). ¹³C NMR (100 MHz, CDCl₃): δ 168.5, 161.2, 143.2, 136.8, 133.0, 130.3, 129.1, 128.4, 126.0, 124.9, 115.4, 108.8, 70.2, 52.6, 46.0, 30.0, 24.1. HRMS calcd for C₂₇H₂₄ClNO₄ [M + H]⁺ 462.1467; found: 462.1466.

2-Chloro-3'-((2-cyclopentyl-1-oxoisindolin-5-yloxy)methyl)biphenyl-4-carboxylic Acid (15e). White solid (14 mg, 15%). ¹H NMR (400 MHz, DMSO-*d*₆): δ 8.00 (s, 1H), 7.94–7.91 (m, 1H), 7.55–7.51 (m, 5H), 7.45–7.43 (m, 1H), 7.21–7.09 (m, 2H), 5.25 (s, 2H), 4.55–4.47 (m, 1H), 4.37 (s, 2H), 1.86–1.56 (m, 8H). ¹³C NMR (100 MHz, DMSO-*d*₆): δ 167.1, 166.0, 160.9, 143.9, 137.0, 131.8, 130.4, 128.6, 128.2, 123.9, 115.3, 109.1, 69.3, 51.9, 45.2, 29.6, 23.8. HRMS calcd for C₂₇H₂₄ClNO₄ [M + H]⁺ 462.1467; found: 462.1464.

3'-((2-Cyclopentyl-1-oxoisindolin-5-yloxy)methyl)-6-methylbiphenyl-3-carboxylic Acid (15f). White solid (15 mg, 32%). ¹H NMR (400 MHz, CDCl₃): δ 7.84–7.80 (m, 2H), 7.60–7.25 (m, 6H), 7.07–7.02 (m, 2H), 5.17 (s, 2H), 4.64–4.57 (m, 1H), 4.31 (s, 2H), 2.26 (s, 3H), 1.91–1.62 (m, 8H). ¹³C NMR (100 MHz, CDCl₃): δ 167.8, 167.6, 161.2, 143.4, 141.1, 141.0, 140.1, 136.4, 130.3, 128.8, 128.6, 128.4, 128.3, 127.9, 126.1, 125.8, 124.1, 115.3, 108.7, 69.8, 52.2, 45.8, 29.8, 23.9, 20.5. LRMS calcd for C₂₈H₂₇NO₄ [M + H]⁺ 442 found: 442. HRMS calcd for C₂₈H₂₇NO₄ [M + H]⁺ 442.2013 found: 442.2000.

3'-((2-Cyclopentyl-1-oxoisindolin-5-yloxy)methyl)-5-fluorobiphenyl-3-carboxylic Acid (15g). White solid (9 mg, 27%). ¹H NMR (400 MHz, DMSO-*d*₆): δ 8.05 (s, 1H), 7.85–7.51 (m, 7H), 7.24–7.11 (m, 2H), 5.28 (s, 2H), 4.56–4.48 (m, 1H), 4.39 (s, 2H), 1.87–1.57 (m, 8H). ¹³C NMR (100 MHz, DMSO-*d*₆): δ 166.8, 160.9, 144.0, 137.6, 129.3, 127.7, 126.5, 126.3, 125.5, 123.9, 123.3, 115.3, 109.1, 69.4, 51.9, 45.6, 29.6, 23.8. HRMS calcd for C₂₇H₂₄FNO₄ [M + H]⁺ 446.1762; found: 446.1767.

3'-((2-Cyclopentyl-1-oxoisindolin-5-yloxy)methyl)-4-methoxybiphenyl-3-carboxylic Acid (15h). White solid (12 mg, 21%).

^1H NMR (400 MHz, CDCl_3): δ 8.45 (s, 1H), 7.81–7.39 (m, 7H), 7.15–7.01 (m, 2H), 5.17 (s, 2H), 4.76–4.70 (m, 1H), 4.29 (s, 2H), 4.12 (s, 3H), 1.99–1.57 (m, 8H). ^{13}C NMR (100 MHz, CDCl_3): δ 168.3, 165.2, 161.4, 157.5, 143.3, 139.5, 137.2, 134.9, 133.4, 132.2, 129.6, 126.3, 125.8, 124.9, 117.9, 115.3, 112.2, 108.7, 70.19, 56.9, 52.5, 45.9, 30.0, 24.1. HRMS calcd for $\text{C}_{28}\text{H}_{27}\text{NO}_5$ [$\text{M} + \text{H}$] $^+$ 458.1962; found: 458.1954.

5-(Biphenyl-3-ylmethoxy)-2-cyclopentylisoindolin-1-one (15i). Pale yellow solid (18 mg, 26%). ^1H NMR (400 MHz, $\text{DMSO}-d_6$): δ 7.75 (s, 1H), 7.68–7.35 (m, 9H), 7.23 (d, $J = 2.3$ Hz, 1H), 7.13–7.11 (m, 1H), 5.26 (s, 2H), 4.56–4.48 (m, 1H), 4.38 (s, 2H), 1.87–1.57 (m, 8H). ^{13}C NMR (100 MHz, $\text{DMSO}-d_6$): δ 166.9, 161.0, 144.0, 140.4, 139.9, 137.4, 129.2, 128.9, 127.6, 126.8, 126.7, 126.3, 126.1, 125.5, 123.9, 115.3, 109.1, 69.5, 51.9, 45.6, 29.6, 23.8. HRMS calcd for $\text{C}_{26}\text{H}_{25}\text{NO}_2$ [$\text{M} + \text{H}$] $^+$ 384.1958; found: 384.1937.

5-((4'-Chloro-2'-fluorobiphenyl-3-yl)methoxy)-2-cyclopentylisoindolin-1-one (15j). Yellow oil (50 mg, 32%). ^1H NMR (400 MHz, $\text{DMSO}-d_6$): δ 7.62–7.51 (m, 7H), 7.41–7.38 (m, 1H), 7.22–7.09 (m, 2H), 5.25 (s, 2H), 4.55–4.47 (m, 1H), 4.38 (s, 2H), 1.84–1.57 (m, 8H). ^{13}C NMR (100 MHz, $\text{DMSO}-d_6$): δ 167.1, 160.9, 144.0, 137.2, 134.2, 131.9, 128.9, 127.9, 127.5, 125.2, 123.9, 116.8, 116.6, 115.3, 109.1, 69.3, 51.9, 45.6, 29.6, 23.8. HRMS calcd for $\text{C}_{26}\text{H}_{23}\text{ClFNO}_2$ [$\text{M} + \text{H}$] $^+$ 436.1474 found: 436.1458.

2-Cyclopentyl-5-((2'-fluoro-4'-(trifluoromethyl)biphenyl-3-yl)methoxy)isoindolin-1-one (15k). Pale yellow solid (25 mg, 23%). ^1H NMR (400 MHz, $\text{DMSO}-d_6$): δ 7.80–7.53 (m, 8H), 7.22–7.09 (m, 2H), 5.25 (s, 2H), 4.54–4.47 (m, 1H), 4.37 (s, 2H), 1.85–1.56 (m, 8H). ^{13}C NMR (100 MHz, $\text{DMSO}-d_6$): δ 166.9, 160.9, 144.0, 137.3, 133.8, 132.1, 129.0, 128.6, 128.1, 125.6, 123.9, 121.8, 115.3, 109.1, 69.3, 51.9, 45.6, 29.6, 23.8. HRMS calcd for $\text{C}_{27}\text{H}_{23}\text{F}_4\text{NO}_2$ [$\text{M} + \text{H}$] $^+$ 470.1738 found: 470.1713.

3'-((2-Cyclopentyl-3-oxo-2,3-dihydrobenzo[d]isothiazol-6-yloxy)methyl)-6-methylbiphenyl-3-carboxylic Acid (16a). A mixture of 3'-((2-cyclopentyl-3-oxo-2,3-dihydrobenzo[d]isothiazol-6-yloxy)methyl)phenylboronic acid (50 mg, 0.14 mmol), 3-iodo-4-methylbenzoic acid (53 mg, 0.20 mmol), and tetrakis(triphenylphosphine)palladium(0) (0.016 mg, 0.014 mmol) were dissolved in DME (2 mL). To this solution was added 1 M Na_2CO_3 (0.48 mmol), and the resulting mixture was heated at reflux under an atmosphere of N_2 for 12 h. The reaction mixture was cooled to room temperature, and the solvents were removed in vacuo. The solvents were evaporated, and the residue was dissolved in water and neutralized using 1 M HCl. The aqueous layer was extracted with ethyl acetate, and the organic layer was dried over anhydrous Na_2SO_4 . The solvent was evaporated in vacuo to obtain the crude acid as a yellow solid. The crude residue was purified using automated preparative HPLC to yield the desired compound as a pale yellow solid (23 mg, 36%). ^1H NMR (400 MHz, CDCl_3): δ 8.01 (s, 1H), 7.90 (d, 1H, $J = 8.5$ Hz), 7.65–7.23 (m, 7H), 7.03 (s, 1H), 5.23 (s, 2H), 4.64–4.59 (m, 1H), 2.34 (s, 3H), 2.16–2.14 (m, 2H), 1.88–1.68 (m, 6H). ^{13}C NMR (100 MHz, CDCl_3): δ 169.9, 165.5, 163.5, 142.2, 141.9, 136.6, 132.6, 132.0, 130.8, 129.3, 128.9, 128.3, 120.2, 110.4, 70.8, 55.8, 24.3, 23.7, 20.9. LC-MS (ESI) Calcd for $\text{C}_{27}\text{H}_{25}\text{NO}_4\text{S}$ [$\text{M} + \text{H}$] $^+$: 460.15. Found: 460.00. HRMS (ESI) Calcd for $\text{C}_{27}\text{H}_{25}\text{NO}_4\text{S}$ [$\text{M} + \text{H}$] $^+$: 460.1577. Found: 460.1565.

2-Cyclopentyl-3-oxo-2,3-dihydrobenzo[d]isothiazol-6-yloxy)methyl)-5-nitrobiphenyl-3-carboxylic Acid (16b). A mixture of 6-(3-bromobenzoyloxy)-2-cyclopentylbenzo[d]isothiazol-3(2H)-one (43 mg, 0.1 mmol), 3-borono-5-nitrobenzoic acid (25 mg, 0.12 mmol), tetrakis(triphenylphosphine)palladium(0) (0.012 mg, 0.028 mmol), and 1 M Na_2CO_3 (2 mmol) were heated in DME at reflux and processed according to the procedure described for 3'-((2-cyclopentyl-3-oxo-2,3-dihydrobenzo[d]isothiazol-6-yloxy)methyl)-6-methylbiphenyl-3-carboxylic acid to afford 3'-((2-cyclopentyl-3-oxo-2,3-dihydrobenzo[d]isothiazol-6-yloxy)methyl)-5-nitrobiphenyl-3-carboxylic acid as a pale yellow solid (23 mg, 47%). ^1H NMR (400 MHz, CDCl_3): δ 8.87 (s, 1H), 8.65 (s, 1H), 8.61 (s, 1H), 7.87 (d, 1H, $J = 8.7$ Hz), 7.71–7.72 (m, 5H), 6.97 (d, 1H, $J = 8.5$ Hz), 5.24 (s, 2H), 4.63–4.59 (m, 1H), 2.19–2.03 (m, 2H), 1.99–1.66 (m, 6H). ^{13}C NMR (100 MHz, CDCl_3): δ 167.5, 165.6, 163.4, 148.8, 143.4, 138.8, 136.0, 134.4, 130.1, 129.8, 128.8,

128.2, 127.2, 126.5, 123.0, 119.9, 110.4, 70.2, 55.8, 32.3, 23.7. LC-MS (ESI) Calcd for $\text{C}_{26}\text{H}_{22}\text{N}_2\text{O}_6\text{S}$ [$\text{M} + \text{H}$] $^+$: 491.11. Found: 491.00. HRMS (ESI) Calcd for $\text{C}_{26}\text{H}_{22}\text{N}_2\text{O}_6\text{S}$ [$\text{M} + \text{Na}$] $^+$: 512.1013. Found: 512.0889.

3'-((2-Cyclopentyl-3-oxo-2,3-dihydrobenzo[d]isothiazol-6-yloxy)methyl)-4-fluorobiphenyl-3-carboxylic Acid (16c). A mixture of 6-(3-bromobenzoyloxy)-2-cyclopentylbenzo[d]isothiazol-3(2H)-one (113 mg, 0.28 mmol), 5-borono-2-fluorobenzoic acid (63 mg, 0.34 mmol), tetrakis(triphenylphosphine)palladium(0) (0.032 mg, 0.028 mmol), and 1 M Na_2CO_3 (2 mmol) were heated in DME at reflux and processed according to the procedure described for 3'-((2-cyclopentyl-3-oxo-2,3-dihydrobenzo[d]isothiazol-6-yloxy)methyl)-6-methylbiphenyl-3-carboxylic acid to afford 3'-((2-cyclopentyl-3-oxo-2,3-dihydrobenzo[d]isothiazol-6-yloxy)methyl)-4-fluorobiphenyl-3-carboxylic acid as a pale yellow solid (54 mg, 42%). ^1H NMR (400 MHz, CDCl_3): δ 8.23 (s, 1H), 7.86 (d, 1H, $J = 8.7$ Hz), 7.61 (s, 1H), 7.57–7.41 (m, 4H), 7.28–7.23 (m, 2H), 7.04 (d, 1H, $J = 8.7$ Hz), 5.25 (s, 2H), 4.61–4.59 (m, 1H), 2.19–2.02 (m, 2H), 1.99–1.65 (m, 6H). ^{13}C NMR (100 MHz, CDCl_3): δ 167.5, 165.6, 163.5, 147.9, 139.7, 137.7, 136.2, 135.6, 131.3, 129.6, 127.5, 127.3, 127.0, 126.2, 121.2, 117.8, 110.4, 70.8, 55.8, 32.2, 23.7. LC-MS (ESI) Calcd for $\text{C}_{26}\text{H}_{22}\text{FNO}_4\text{S}$ [$\text{M} + \text{H}$] $^+$: 464.12. Found: 463.95. HRMS (ESI) Calcd for $\text{C}_{26}\text{H}_{22}\text{FNO}_4\text{S}$ [$\text{M} + \text{H}$] $^+$: 464.1326. Found: 464.1304.

6-(3-Bromobenzoyloxy)-2-cyclopentylbenzo[d]isothiazol-3(2H)-one (18). Potassium carbonate (94 mg, 0.66 mmol) was added to a solution of 2-cyclopentyl-7-hydroxy-3,4-dihydroisoquinolin-1(2H)-one (132 mg, 0.56 mmol) and 1-bromo-3-(bromomethyl)benzene (164 mg, 0.66 mmol) in CH_3CN (10 mL). After being stirred for 1 h at 80 °C, the organic phase was evaporated under reduced pressure, and the crude material was partitioned between water and CH_2Cl_2 . The aqueous layer was extracted with CH_2Cl_2 (3 \times 15 mL). The organic phase was dried using Na_2SO_4 and evaporated to give 6-(3-bromobenzoyloxy)-2-cyclopentylbenzo[d]isothiazol-3(2H)-one (223 mg, 98%). The crude product was used for the next step without further purification. ^1H NMR (400 MHz, CDCl_3): δ 7.90 (d, 1H, $J = 9.6$ Hz), 7.58 (s, 1H), 7.48 (d, 1H, $J = 8.2$ Hz), 7.33 (d, 1H, $J = 7.8$ Hz), 7.25 (t, 1H, $J = 7.7$ Hz), 7.00–6.99 (overlapping singlet and doublet, 2H), 5.09 (s, 2H), 5.04–5.02 (m, 1H), 2.16–2.13 (m, 2H), 1.84–1.67 (m, 6H). ^{13}C NMR (100 MHz, CDCl_3): δ 165.3, 162.3, 142.1, 138.4, 131.4, 130.4, 127.8, 125.9, 114.9, 104.3, 69.6, 55.1, 32.2, 24.4. LC-MS (ESI) Calcd for $\text{C}_{19}\text{H}_{18}\text{BrNO}_2$ [$\text{M} + \text{H}$] $^+$: 404.02, 406.02. Found: 403.90, 405.80.

4-Chloro-3'-((2-cyclopentyl-3-oxo-2,3-dihydrobenzo[d]isothiazol-6-yloxy)methyl)-N,N-methylbiphenyl-3-carboxamide (19). The acid (48 mg, 0.1 mmol) was dissolved in DMF (2 mL) at room temperature. HOBT (16 mg, 0.12 mmol) was added in one portion followed by EDC-HCl (23 mg, 0.12 mmol). The resulting mixture was stirred at room temperature for 30 min. To this solution were added dimethylamine hydrochloride (10 mg, 0.12 mmol) and triethylamine (0.02 mL, 0.12 mmol), the mixture was stirred for 2 h, and the organic phase was evaporated under reduced pressure. The crude material was partitioned between water and ethyl acetate, and the aqueous layer was extracted with ethyl acetate (3 \times 5 mL). The organic phase was dried using Na_2SO_4 and evaporated to give 4-chloro-3'-((2-cyclopentyl-3-oxo-2,3-dihydrobenzo[d]isothiazol-6-yloxy)methyl)-N,N-dimethylbiphenyl-3-carboxamide. The crude product was purified by HPLC using 2-propanol:water as the solvent system to afford the amide as a colorless solid (40 mg, 80% yield). ^1H NMR (400 MHz, CDCl_3): δ 7.87 (d, 1H, $J = 8.7$ Hz), 7.60 (s, 1H), 7.75–7.38 (m, 4H), 7.27–7.24 (m, 3H), 7.03 (d, 1H, $J = 8.5$ Hz), 5.25 (s, 2H), 4.63–4.59 (m, 1H), 3.15 (s, 3H), 2.91 (s, 3H), 2.16–2.03 (m, 2H), 1.62–1.60 (m, 6H). ^{13}C NMR (100 MHz, CDCl_3): δ 168.4, 165.6, 163.5, 147.9, 140.0, 137.7, 136.6, 130.1, 129.6, 128.8, 127.5, 127.3, 127.1, 126.5, 126.1, 115.5, 110.2, 70.6, 55.8, 38.2, 34.9, 32.2. LC-MS (ESI) Calcd for $\text{C}_{28}\text{H}_{27}\text{ClNO}_3\text{S}$ [$\text{M} + \text{H}$] $^+$: 507.14. Found: 507.05. HRMS (ESI) Calcd for $\text{C}_{28}\text{H}_{27}\text{ClNO}_3\text{S}$ [$\text{M} + \text{H}$] $^+$: 507.1504. Found: 507.1519.

5-Bromo-2-cyclopentylisoindolin-1-one (23). ^1H NMR (400 MHz, CDCl_3): δ 7.63–7.51 (m, 3H), 4.71–4.63 (m, 1H), 4.29 (s, 2H), 1.97–1.54 (m, 8H). LRMS calcd for $\text{C}_{13}\text{H}_{14}\text{BrNO}$ [$\text{M} + \text{H}$] $^+$ 280 found: 280.

4-Chloro-3'-(2-cyclopentyl-1-oxoisindolin-5-yl)biphenyl-3-carboxylic Acid (24). A solution of 3-bromophenylboronic acid (134 mg, 0.67 mmol) and 5-bromo-2-cyclopentylisindolin-1-one (187 mg, 0.67 mmol) in DME (3.5 mL) was treated with 2 M Na₂CO₃ (1.7 mL, 3.35 mmol) and Pd(PPh₃)₄ (14 mg, 0.012 mmol) and heated at reflux under an atmosphere of N₂ for 1 h to obtain 5-(3-bromophenyl)-2-cyclopentylisindolin-1-one. The reaction mixture was cooled, treated with 5-bromo-2-chlorobenzoic acid (671 mg, 3.35 mmol), 2 M Na₂CO₃ (1.7 mL, 3.35 mmol), DME (3.5 mL), and Pd(PPh₃)₄ (14 mg, 0.012 mmol), and heated at reflux under an atmosphere of N₂ for 1.5 h. The mixture was cooled and filtered through Celite, and the solvent was evaporated in vacuo. The residue was acidified with 2 M HCl, and the resulting crude acid was purified using automated preparative HPLC to yield the desired product (34.5 mg, 12% over two steps) as a pale yellow solid. ¹H NMR (400 MHz, CDCl₃): δ 8.24 (d, *J* = 2.3 Hz, 1H), 7.94 (d, *J* = 8.0 Hz, 1H), 7.78–7.54 (m, 8H), 4.84–4.75 (m, 1H), 4.43 (s, 2H), 2.08–2.00 (m, 2H), 1.83–1.62 (m, 6H). ¹³C NMR (100 MHz, CDCl₃): δ 168.4, 144.0, 141.9, 141.5, 139.6, 133.6, 132.5, 131.7, 130.8, 129.7, 127.5, 127.2, 126.5, 126.2, 124.1, 121.5, 52.7, 46.2, 30.1, 24.1. HRMS calcd for C₂₆H₂₂ClNO₃ [M + H]⁺ 432.1361 found: 432.1363.

mGlu₂ Receptor in Vitro Assay. Human embryonic kidney (HEK-293) cell lines coexpressing rat mGlu receptors 2, 3, 4, 6, 7, or 8 and G protein inwardly rectifying potassium (GIRK) channels²⁵ were grown in growth media containing 45% DMEM, 45% F-12, 10% FBS, 20 mM HEPES, 2 mM L-glutamine, antibiotic/antimycotic, non-essential amino acids, 700 μg/mL G418, and 0.6 μg/mL puromycin at 37 °C in the presence of 5% CO₂. Cells expressing rat mGlu₁ and mGlu₅ receptors were cultured as described in Hemstapat et al.²⁷ All cell culture reagents were purchased from Invitrogen Corp. (Carlsbad, CA) unless otherwise noted. Calcium assays were used to assess activity of compounds at mGlu₁ and mGlu₅, as previously described in Engers et al.²⁸ Compound activity at the group II (mGlu₂ and mGlu₃) and group III (mGlu₄, mGlu₆, mGlu₇, and mGlu₈) receptors was assessed using thallium flux through GIRK channels, a method that has been described in detail.²⁵ Briefly, cells were plated into 384-well, black-walled, clear-bottomed poly-D-lysine-coated plates at a density of 15 000 cells/20 μL/well in DMEM containing 10% dialyzed FBS, 20 mM HEPES, and 100 units/mL penicillin/streptomycin (assay media). Plated cells were incubated overnight at 37 °C in the presence of 5% CO₂. The following day the medium was exchanged from the cells to assay buffer [Hanks balanced salt solution (Invitrogen) containing 20 mM HEPES, pH 7.3] using an ELX405 microplate washer (BioTek), leaving 20 μL/well, followed by the addition of 20 μL/well FluoZin2-AM (330 nM final concentration) indicator dye (Invitrogen; prepared as a stock in DMSO and mixed in a 1:1 ratio with Pluronic acid F-127) in assay buffer. Cells were incubated for 1 h at room temperature, and the dye was exchanged to assay buffer using an ELX405, leaving 20 μL/well. Test compounds were diluted to 2 times their final desired concentration in assay buffer (0.3% DMSO final concentration). Agonists were diluted in thallium buffer [125 mM sodium bicarbonate (added fresh the morning of the experiment), 1 mM magnesium sulfate, 1.8 mM calcium sulfate, 5 mM glucose, 12 mM thallium sulfate, and 10 mM HEPES, pH 7.3] at 5 times the final concentration to be assayed. Cell plates and compound plates were loaded onto a kinetic imaging plate reader (FDSS 6000 or 7000; Hamamatsu Corporation, Bridgewater, NJ). Appropriate baseline readings were taken (10 images at 1 Hz; excitation, 470 ± 20 nm; emission, 540 ± 30 nm), and test compounds were added in a 20 μL volume and incubated for approximately 2.5 min before the addition of 10 μL of thallium buffer with or without agonist. After the addition of agonist, data were collected for approximately an additional 2.5 min. Data were analyzed using Excel (Microsoft Corp, Redmond, WA). The slope of the fluorescence increase beginning 5 s after thallium/agonist addition and ending 15 s after thallium/agonist addition was calculated, corrected to vehicle and maximal agonist control slope values, and plotted using either XLfit (ID Business Solutions Ltd.) or Prism software (GraphPad Software, San Diego, CA) to generate concentration–response curves. Potencies were calculated from fits using a four-point parameter logistic equation. For concentration–response curve experiments, compounds were serially diluted 1:3 into 10 point concentration–response curves and were transferred to daughter

plates using an Echo acoustic plate reformatter (Labcyte, Sunnyvale, CA). Test compounds were applied and followed by EC₂₀ concentrations of glutamate. For selectivity experiments, full concentration–response curves of glutamate or L-AP4 (for mGlu₇) were performed in the presence of a 10 μM concentration of compound, and compounds that affected the concentration–response by less than 2 fold in terms of potency or efficacy were designated as inactive.

Microsomal Stability in Vitro Assay. Pooled rat liver microsomes (BD Biosciences, # 452701) were preincubated with test compounds at 37.5 °C for 5 min in the absence of NADPH. The reaction was initiated by addition of NADPH and incubated under the same conditions. The final incubation concentrations were 4 μM test compound, 2 mM NADPH, and 1 mg/mL (total protein) liver microsomes in phosphate-buffered saline (PBS) at pH 7.4. One aliquot (100 μL) of the incubation mixture was withdrawn at 15 min time points and combined immediately with 100 μL of ACN/MeOH. After mixing, the sample was centrifuged at approximately 13 000 rpm for 12 min. The supernatant was filtered and transferred into an autosampler vial, and the amount of test compound was quantified using a Shimadzu LCMS 2010EV mass spectrometer. The change of the AUC (area under the curve) of the parent compound as a function of time was used as a measure of microsomal stability. Test compounds were run in duplicate with a positive control.

Plasma Stability in Vitro Assay. A 20 μL aliquot of a 10 mM solution in DMSO of the test compound was added to 2.0 mL of heparinized rat plasma (Lampire, P1-150N) to obtain a 100 μM final solution. The mixture was incubated for 1 h at 37.5 °C. Aliquots of 100 μL were taken at 15 min intervals and diluted with 100 μL of MeOH/ACN. After mixing, the sample was centrifuged at approximately 13 000 rpm for 12 min. The supernatant was filtered and transferred into an autosampler vial, and the amount of test compound was quantified using the Shimadzu LCMS-2010EV system. The change of the AUC of the parent compound as a function of time was used as a measure of plasma stability.

Parallel Artificial Membrane Permeation Assay (PAMPA). A 96-well microtiter plate (Millipore, # MSSACCEPTOR) was completely filled with aqueous buffer solution (pH 7.4) and covered with a microtiter filterplate (Millipore, # MAPBMN310) to create a sort of sandwich construction.²⁶ The hydrophobic filter material was impregnated with a 10% solution of polar brain lipid extract in chloroform (Avanti, Alabaster, AL) as the artificial membrane, and the organic solvent was allowed to completely evaporate. Permeation studies were started by the transfer of 200 μL of a 100 μM test compound solution on top of the filter plate. In general, phosphate pH 7.2 buffer was used. The maximum DMSO content of the stock solutions was <1.5%. In parallel, an equilibrium solution lacking a membrane was prepared using the exact concentrations and specifications but lacking the membrane. The concentrations of the acceptor and equilibrium solutions were determined using the Shimadzu LCMS-2010EV and AUC methods. The Acceptor plate and equilibrium plate concentrations were used to calculate the permeability rate (log *P_e*) of the compounds. The log *P_e* values were calculated using the following equation:

$$\log P_e = \log \left\{ C \times - \ln \left(1 - \frac{[\text{drug}]_{\text{acceptor}}}{[\text{drug}]_{\text{equilibrium}}} \right) \right\}$$

where *V_D* and *V_A* are the volumes of the donor and acceptor compartments

$$C = (V_D \times V_A) / ((V_D + V_A) \text{area} \times \text{time})$$

Assays Measuring Inhibition of Drug-Metabolizing Enzymes CYP1A2, CYP2C9, and CYP3A4. Evaluation of the compounds as inhibitors of the activity of CYP1A2, CYP2C9, or CYP3A4 was assessed using the P450-Glo CYP1A2 Assay kit (Promega, P/N V8422), the CYP2C9 Assay kit (Promega, P/N V8792), or the CYP3A4 Assay kit (Promega, P/N V8912) in the presence of human liver microsomes (XenoTech, P/N H0610, lot # 0810509). NADPH, a required cofactor for CYP450 metabolism, was provided by the NADPH Regenerating System, Solutions A (BD Biosciences, P/N 451220) and B (BD Biosciences, P/N 451200). Compound stock solutions were initially prepared in 100% DMSO and subsequently diluted in acetonitrile for

the assay. The pH of the reactions was maintained at ~7.4 with potassium phosphate buffer (BD Biosciences, P/N 451201). The reaction was started after adding NADPH and the corresponding CYP substrates (luciferin-1A2 for CYP1A2, luciferin-H for CYP2C9, or luciferin-PPXE for CYP3A4) to the reaction plate containing microsomes and compounds. The reaction was incubated for 10 min (CYP1A2), 30 min (CYP2C9), or 20 min (CYP3A4) at 37 °C with shaking. The Luciferin Detection Reagent was added after the incubation to stop the reaction and initiate a stable glow-type luminescent signal. The luminescence of the metabolite that was formed, luciferin, was recorded with the Infinite M200 (Tecan US). All reactions were run in duplicate, except negative controls (no NADPH) which were performed as single reactions. The background luminescence obtained from the negative control reactions was subtracted from the luminescence values obtained for the positive reaction duplicates.

Behavioral Procedures. *Apparatus.* Intravenous nicotine self-administration took place in 24 Plexiglas experimental chambers (25 × 31 × 24 cm; MED Associates, St. Albans, VT), each housed in a sound-attenuating box (San Diego Instruments, San Diego, CA). One wall of the chamber contained two levers, measuring approximately 3 cm in width and located approximately 3 cm above the metal grid floor of the chamber. There was also an opaque disk (2.5 cm diameter) mounted 10 cm above each lever which could be illuminated by a 2.5 W, 24 V white light bulb and served as a cue light paired with nicotine delivery. All data collection and test session functions were controlled by computers and MED-PC IV software (MED Associates).

Nicotine Self-Administration Procedure. Catheter construction and surgery and the nicotine self-administration procedure were performed as described previously.^{8,14} Briefly, rats were initially trained to press a lever using food as a reward. Subsequently a jugular venous catheter was surgically inserted using isoflurane anesthesia (1–1.5% isoflurane/oxygen mixture). After one week of recovery from surgery, the animals were allowed to self-administer nicotine (0.03 mg/kg/infusion) during 1 h self-administration sessions. Self-administration sessions were initiated by extension of the two levers (active and inactive) in the chamber. Every five responses (FR5) on the active lever resulted in the delivery of a single infusion of nicotine (0.1 mL over 1 s). Each infusion of nicotine was paired with the presentation of a cue light located above the active lever for the duration of the infusion and for a period of 20 s termed the timeout period. During the timeout period responses on the active lever did not result in delivery of nicotine infusions. Responses on the inactive lever were recorded but did not result in any nicotine infusions. All rats were trained to self-administer nicotine for 3 weeks (5 days/week). All animals showed stable nicotine self-administration behavior over the three weeks of self-administration training (more than six infusions per session with less than 20% variation over three consecutive sessions).

Experimental Design for Investigating the Effects of the mGlu₂ Receptor PAM on Nicotine Self-Administration. After completion of the nicotine self-administration training, drug treatments were initiated. Compound 2 was administered to rats ($n = 7$) according to a within-subjects Latin-square design. The compound was administered orally at doses of 0, 10, and 20 mg/kg 2 h prior to nicotine self-administration sessions (pretreatment time). This pretreatment time was selected based on the PK data (see Tables 5 and 6). At least three days elapsed between drug/vehicle injections to re-establish stable self-administration behavior (less than 20% variation over three days).

Statistical Analyses. Intravenous nicotine self-administration data were expressed as a percentage of the baseline number of rewards earned, with baseline defined as the mean number of rewards earned during the three days before each drug testing session. Data were expressed as percent values, as each animal served as its own control and conversion of data into percent of baseline best represented the data. Identical results were obtained when the data were analyzed as raw values. Acute effects of compound 2 on nicotine self-administration were analyzed using one-way repeated-measures ANOVA, and posthoc comparisons were conducted with the Newman–Keuls tests. The criterion for significance was set at 0.05.

A one-way ANOVA showed a significant main effect of dose ($F_{(2, 12)} = 6.81$; $p < 0.01$). Newman–Keuls posthoc test showed a

significant dose-dependent decrease in nicotine self-administration after administration of compound 2 at 10 ($p < 0.05$) and 20 mg/kg ($p < 0.01$) compared to vehicle treatment.

AUTHOR INFORMATION

Corresponding Author

*Tel: 858-646-3100. Fax: 858-795-5225. E-mail: ncosford@sanfordburnham.org.

Author Contributions

[†]These authors contributed equally to this work.

Notes

The authors declare no competing financial interest.

ACKNOWLEDGMENTS

This work was supported by National Institutes of Health grant R01 DA023926 to N.C., and DA011946 to A.M. The binding profiles for compounds 2 and 3 were generously provided by the National Institute of Mental Health's Psychoactive Drug Screening Program, contract # HHSN-271-2008-00025-C (NIMH PDSP).

ABBREVIATIONS USED

mGlu₂ receptor, metabotropic glutamate receptor subtype 2; PAM, positive allosteric modulator; BINA, 3'-((2-cyclopentyl-6,7-dimethyl-1-oxo-2,3-dihydro-1H-inden-5-yloxy)methyl)-biphenyl-4-carboxylic acid; HTS, high-throughput screening; PK, pharmacokinetic; PIFA, phenyliodine bis(trifluoroacetate); EDC, 1-ethyl-3-(3-dimethylaminopropyl)carbodiimide; AIBN, 2,2'-azobis(isobutyronitrile); NBS, N-bromosuccinimide; HEK, human embryonic kidney; GIRK, G protein inwardly rectifying potassium; PBS, phosphate-buffered saline; DMEM, Dulbecco's modified eagle medium; HEPES, 4-(2-hydroxyethyl)-1-piperazineethanesulfonic acid; FBS, fetal bovine serum

REFERENCES

- (1) World Health Organization. *WHO Report on the Global Tobacco Epidemic*; World Health Organization: Geneva, 2008.
- (2) Centers for Disease Control and Prevention. Current cigarette smoking prevalence among working adults: United States, 2004–2010. *Morbidity and Mortality Weekly Report* **2011**, *60*, 1305–1309.
- (3) Agboola, S.; McNeill, A.; Coleman, T.; Leonardi Bee, J. A systematic review of the effectiveness of smoking relapse prevention interventions for abstinent smokers. *Addiction* **2010**, *105*, 1362–1380.
- (4) Stolerman, I. P.; Jarvis, M. J. The scientific case that nicotine is addictive. *Psychopharmacology (Berlin, Ger.)* **1995**, *117*, 2–10; discussion 14–20.
- (5) Liechti, M. E.; Markou, A. Role of the glutamatergic system in nicotine dependence: implications for the discovery and development of new pharmacological smoking cessation therapies. *CNS Drugs* **2008**, *22*, 705–724.
- (6) Markou, A. Neurobiology of nicotine dependence. *Philos. Trans R. Soc. London, Ser. B* **2008**, *363*, 3159–3168.
- (7) D'Souza, M. S.; Markou, A. Neuronal mechanisms underlying development of nicotine dependence: implications for novel smoking-cessation treatments. *Addict. Sci. Clin. Pract.* **2011**, *6*, 4–16.
- (8) D'Souza, M. S.; Liechti, M. E.; Ramirez-Nino, A. M.; Kuczenski, R.; Markou, A. The metabotropic glutamate 2/3 receptor agonist LY379268 blocked nicotine-induced increases in nucleus accumbens shell dopamine only in the presence of a nicotine-associated context in rats. *Neuropsychopharmacology* **2011**, *36*, 2111–2124.
- (9) Cartmell, J.; Schoepp, D. D. Regulation of neurotransmitter release by metabotropic glutamate receptors. *J. Neurochem.* **2000**, *75*, 889–907.
- (10) Xi, Z. X.; Baker, D. A.; Shen, H.; Carson, D. S.; Kalivas, P. W. Group II metabotropic glutamate receptors modulate extracellular

glutamate in the nucleus accumbens. *J. Pharmacol. Exp. Ther.* **2002**, *300*, 162–171.

(11) Xi, Z. X.; Ramamoorthy, S.; Baker, D. A.; Shen, H.; Samuvel, D. J.; Kalivas, P. W. Modulation of group II metabotropic glutamate receptor signaling by chronic cocaine. *J. Pharmacol. Exp. Ther.* **2002**, *303*, 608–615.

(12) Kalivas, P. W. The glutamate homeostasis hypothesis of addiction. *Nat. Rev. Neurosci.* **2009**, *10*, 561–572.

(13) Semenova, S.; Markou, A. Metabotropic glutamate receptors as targets for the treatment of drug and alcohol dependence. In *Glutamate-based Therapies for Psychiatric Disorders*; Skolnick, P., Vol. Ed.; Parnham, M.J.; Bruinvels, J., Series Eds.; *Milestones in Drug Therapy*; Springer Birkhauser: Basel, 2010; pp 133–156.

(14) Liechti, M. E.; Lhuillier, L.; Kaupmann, K.; Markou, A. Metabotropic glutamate 2/3 receptors in the ventral tegmental area and the nucleus accumbens shell are involved in behaviors relating to nicotine dependence. *J. Neurosci.* **2007**, *27*, 9077–9085.

(15) Conn, P. J.; Pin, J. P. Pharmacology and functions of metabotropic glutamate receptors. *Annu. Rev. Pharmacol. Toxicol.* **1997**, *37*, 205–237.

(16) Sheffler, D. J.; Pinkerton, A. B.; Dahl, R.; Markou, A.; Cosford, N. D. P. Recent progress in the synthesis and characterization of group II metabotropic glutamate receptor allosteric modulators. *ACS Chem. Neurosci.* **2011**, *2*, 382–393.

(17) Fell, M. J.; Witkin, J. M.; Falcone, J. F.; Katner, J. S.; Perry, K. W.; Hart, J.; Rorick-Kehn, L.; Overshiner, C. D.; Rasmussen, K.; Chaney, S. F.; Benvenga, M. J.; Li, X.; Marlow, D. L.; Thompson, L. K.; Luecke, S. K.; Wafford, K. A.; Seidel, W. F.; Edgar, D. M.; Quets, A. T.; Felder, C. C.; Wang, X.; Heinz, B. A.; Nikolayev, A.; Kuo, M.-S.; Mayhugh, D.; Khilevich, A.; Zhang, D.; Ebert, P. J.; Eckstein, J. A.; Ackermann, B. L.; Swanson, S. P.; Catlow, J. T.; Dean, R. A.; Jackson, K.; Tauscher-Wisniewski, S.; Marek, G. J.; Schkeryantz, J. M.; Svensson, K. A. N-(4-((2-(Trifluoromethyl)-3-hydroxy-4-(isobutyl)-phenoxy) methyl)benzyl)-1-methyl-1H-imidazole-4-carboxamide (THIIC), a novel metabotropic glutamate 2 potentiator with potential anxiolytic/antidepressant properties: in vivo profiling suggests a link between behavioral and central nervous system neurochemical changes. *J. Pharmacol. Exp. Ther.* **2011**, *336*, 165–177.

(18) Garbaccio, R. M.; Brnardic, E. J.; Fraley, M. E.; Hartman, G. D.; Hutson, P. H.; O'Brien, J. A.; Magliaro, B. C.; Uslaner, J. M.; Huszar, S. L.; Fillgrove, K. L.; Small, J. H.; Tang, C.; Kuo, Y.; Jacobson, M. A. Discovery of oxazolobenzimidazoles as positive allosteric modulators for the mGluR2 receptor. *ACS Med. Chem. Lett.* **2010**, *1*, 406–410.

(19) Zhang, L.; Brodney, M. A.; Candler, J.; Doran, A. C.; Duplantier, A. J.; Efremov, I. V.; Evrard, E.; Kraus, K.; Ganong, A. H.; Haas, J. A.; Hanks, A. N.; Jenza, K.; Lazzaro, J. T.; Maklad, N.; McCarthy, S. A.; Qian, W.; Rogers, B. N.; Rottas, M. D.; Schmidt, C. J.; Siuciak, J. A.; Tingley, F. D., III; Zhang, A. Q. 1-[(1-Methyl-1H-imidazol-2-yl)methyl]-4-phenylpiperidines as mGluR2 positive allosteric modulators for the treatment of psychosis. *J. Med. Chem.* **2011**, *54*, 1724–1739.

(20) Cid, J. M.; Duvey, G.; Tresadern, G.; Nhem, V.; Furnari, R.; Cluzeau, P.; de Lucas, A. I.; Matesanz, E.; Alonso, J. M.; Linares, M. L.; Andrés, J. I.; Poli, S. M.; Vega, J. A.; Lutjens, R.; Himogai, H.; Rocher, J.-P.; Macdonald, G. J.; Oehlich, D.; Lavreysen, H.; Ahnaou, A.; Drinkenburg, W.; Mackie, C.; Trabanco, A. A. Discovery of 1,4-disubstituted 3-cyano-2-pyridones: A new class of positive allosteric modulators of the metabotropic glutamate 2 receptor. *J. Med. Chem.* **2012**, *55*, 2388–2405.

(21) Trabanco, A. A.; Tresadern, G.; Macdonald, G. J.; Vega, J. A.; de Lucas, A. I.; Matesanz, E.; García, A.; Linares, M. L.; de Diego, S. A. A.; Alonso, J. M.; Oehlich, D.; Ahnaou, A.; Drinkenburg, W.; Mackie, C.; Andrés, J. I.; Lavreysen, H.; Cid, J. M. Imidazo[1,2-*a*]pyridines: Orally active positive allosteric modulators of the metabotropic glutamate 2 receptor. *J. Med. Chem.* **2012**, *55*, 2688–2701.

(22) Dhanya, R.; Sidique, S.; Sheffler, D. J.; Nickols, H. H.; Herath, A.; Yang, L.; Dahl, R.; Ardecky, R.; Semenova, S.; Markou, A.; Conn, P. J.; Cosford, N. D. P. Design and synthesis of an orally active metabotropic glutamate receptor subtype-2 (mGluR2) positive

allosteric modulator (PAM) that decreases cocaine self-administration in rats. *J. Med. Chem.* **2011**, *54*, 342–353.

(23) Jin, X.; Semenova, S.; Yang, L.; Ardecky, A.; Sheffler, D. J.; Dahl, R.; Conn, P. J.; Cosford, N. D. P.; Markou, M. The mGluR2 positive allosteric modulator BINA decreases cocaine self-administration, cue-induced cocaine-seeking and counteracts cocaine-induced enhancement of brain reward function in rats. *Neuropsychopharmacology* **2010**, *35*, 2021–2036.

(24) Van Wagenen, B.; Ukkirampandian, R.; Clayton, J.; Egle, I.; Empfield, J.; Isaac, M.; Ma, F.; Slassi, A.; Steelman, G.; Urbanek, R.; Walsh, S. Metabotropic glutamate receptor potentiating isoindolones. WO/2007/021308, Feb 22, 2007.

(25) Niswender, C. M.; Johnson, K. A.; Luo, Q.; Ayala, J. E.; Kim, C.; Conn, P. J.; Weaver, C. D. A novel assay of Gi/o-linked G protein-coupled receptor coupling to potassium channels provides new insights into the pharmacology of the group III metabotropic glutamate receptors. *Mol. Pharmacol.* **2008**, *73*, 1213–1224.

(26) Di, L.; Kerns, E. H.; Fan, K.; McConnell, O. J.; Carter, G. T. High throughput artificial membrane permeability assay for blood-brain barrier. *Eur. J. Med. Chem.* **2003**, *38*, 223–232.

(27) Hemstapat, K.; Da Costa, H.; Nong, Y.; Brady, A. E.; Luo, Q.; Niswender, C. M.; Tamagnan, G. D.; Conn, P. J. A novel family of potent negative allosteric modulators of group II metabotropic glutamate receptors. *J. Pharmacol. Exp. Ther.* **2007**, *322*, 254–264.

(28) Engers, D. W.; Niswender, C. M.; Weaver, C. D.; Jadhav, S.; Menon, U. N.; Zamorano, R.; Conn, P. J.; Lindsley, C. W.; Hopkins, C. R. Synthesis and evaluation of a series of heterobiaryl amides that are centrally penetrant metabotropic glutamate receptor 4 (mGluR4) positive allosteric modulators (PAMs). *J. Med. Chem.* **2009**, *52*, 4115–4118.